

Synthesis and Molecular Docking of 7-Methoxy-2-Phenyl-1-Benzofuran-5-Carbaldehyde

Bapu R. Thorat^{1*}, Ravindra Jagtap², Vaishali B. Thorat³, Annasaheb Khemanar⁴ and Ramesh S. Yamgar⁵

¹ P. G. and Research centre, Ismail Yusuf Arts, Science and Commerce College, Jogeshwari (E), Mumbai 400060.

² JJT University, Rajasthan.

³ IES, Junior College, Bandra (E), Mumbai.

⁴ Institute of Science, Fort, Mumbai

⁵ Patkar Varde College, Goregaon (W), Mumbai.

*Corresponding author: Bapu R. Thorat; e-mail: iycbrthorat@gmail.com

Received: 21 November 2014

Accepted: 16 December 2014

Online: 01 January 2015

ABSTRACT

The 7-methoxy-2-phenyl-1-benzofuran-5-carbaldehyde was synthesised by known literature method (Wittig reaction approach). To deduce the anticancer and antibacterial activity of the 7-methoxy-2-phenyl-1-benzofuran-5-carbaldehyde, it is docked with different biomarkers of cancer cell and bacteria. Grid was generated for each oncoproteins by specifying the active site amino acids. The binding model of best scoring analogue with each protein was assessed from their G-scores and disclosed by docking analysis using the XP visualizer tool. An analysis of the receptor-ligand interaction studies revealed that 7-methoxy-2-phenyl-1-benzofuran-5-carbaldehyde is most active against 1VOM and 4FNY biomarkers and have the features to prove themselves as anticancer drugs.

Keywords: Benzofurans, Molecular docking, Anticancer, 1VOM, 4FNY, Wittig reaction.

1.0 INTRODUCTION

Molecular modelling can accelerate and guide to the chemist or scientist for drug design and contribute to the understanding of the biochemical functions of gene products. These molecular modelling techniques used for the study of organic/inorganic/bio molecules use theoretical and computationally based methods to model or mimic the behaviour of molecule/s and have been widely applied for understanding and predicting the behaviour of molecular systems [1]. Molecular modelling has become an essential part of contemporary drug discovery processes of new molecules. A traditional approach for drug discovery of molecules relies on step-wise synthesis and screening of large numbers of compounds to optimize activity profiles of molecule which is to act as drug; this is extremely time consuming and costly method takes decades of years. The cost of these processes has

increased significantly in recent years [2], and it takes over a decade for a very small fraction of compounds to pass the drug discovery pipeline from initial screening hits or leads, chemical optimization, and clinical trials before launching into the market as drug. The approaches and methodologies used in drug design have changed over time, exploiting and driving new technological advances to solve the varied bottlenecks found along the way. There are several programs used for docking, including DOCK-6, FlexX, GLIDE, GOLD, FRED, and SURFLEX has been assessed and these programs proved to generate reliable poses in numerous docking studies.

Until 1990, the major issues were lead discovery and chemical synthesis of drug-like molecules; the emergence of combinatorial chemistry, [4] gene technology, and high-throughput tests [5, 6] has shifted

the focus, and poor absorption, distribution, metabolism, and excretion (ADME) properties of new drugs captured more attention [7].

Protein docking is a computational problem to predict the binding of a protein with potential interacting partners. The docking problem can be defined as: Given the atomic coordinates of two molecules, predict their correct bound association [3], which is the relative

orientation and position after interaction. There are three key components in protein docking: (1) representation of the molecules, (2) searching and (3) scoring of the potential solutions.

2.0 MATERIALS AND METHODS

Docking software used: Maestro 9.9 (Schrodinger). The selected protein crystal structures are given in Table 1.

Table 1. Protein structures selected for docking.

PDB of protein	Worked as	Source
1YCR	MDM2 bound to the trans-activation domain of p53	Homo sapiens
1Z92	Interleukin-2 with its alpha receptor	Homo sapiens
2b4J	Recognition between hiv-1 integrase and ledgf/p75	Homo sapiens
3F8S	Dipeptidyl peptidase IV (DPP-4) in complex with inhibitor	Homo sapiens
1BAG	Alpha-amylase from bacillus subtilis complexed with maltopentaose	Bacillus subtilis
1RJB (FLT3)	Fl cytokine receptor	Homo sapiens
3FDN	Serine/threonine-protein kinase 6	Homo sapiens
3LAU	Arora 2 kinase	Homo sapiens
4BBG	Human kinesin eg5 -like protein kif11	Homo sapiens
3V3M	3C-like proteinase [severe acute respiratory syndrome coronavirus (sars-cov) 3cl protease]	Homo sapiens
1TE6	Gamma enolase [human neuron specific enolase]	Homo sapiens
1VOM	Dictyostelium myosin	Dictyostelium discoideum
2BOU	EGF domains 1,2,5 of human emr2, a 7-tm immune system molecule	Homo sapiens
3MK2	Placental alkaline phosphatase	Homo sapiens
1KDR	Cytidine monophosphate kinase	Escherichia coli
1P62	Deoxycytidine kinase	Escherichia coli
1UFQ	Uridine-cytidine kinase 2	Homo sapiens
2AZ1	Nucleoside diphosphate kinase	Escherichia coli
4FNY	ALK tyrosine kinase receptor	Homo sapiens

2.1 Protocol for ligand-receptor docking

The three dimensional structures of all proteins were taken from the PDB database. The native autoinducer and all water molecules were removed from basic protein structures. Hydrogen were added using the templates for the protein residues. The three-dimensional structure of the ligand (7-methoxy-2-phenyl-1-benzofuran-5-carbaldehyde) was constructed. The ligand was then energy-minimized in the in-built ChemSketch module of the software.

2.2 Docking

The active site of each protein were first identified and defined using an eraser size of 5.0 Å. The ligand was docked into the active site separately using the 'Flexible Fit' option. The ligand-receptor site complex was subjected to 'in situ' ligand minimization which was performed using the in-built CHARMM forcefield calculation. The nonbond cutoff and the distance dependence was set to 11 Å and ($\epsilon = 1R$) respectively. The determination of the ligand binding affinity was calculated using the shape-based interaction energies of the ligand with the protein. Consensus scoring with the top tier of $s=10\%$ using docking score used to estimate the ligand-binding energies.

2.3 Experimental Work

7-Methoxy-2-phenyl-1-benzofuran-5-carbaldehyde is synthesised by known literature method [8]. A mixture of phosphonium salt (1.5 g, 0.0032 mol), benzoyl

chloride (0.5 g, 0.0032 mol) and triethylamine (0.74 g, 0.0073 mol) in 30 ml toluene was heated under reflux for about 6 hr. The reaction mixture was cooled to room temperature and added 20 ml cold water. The organic layer was separated, washed with water and dried by using anhydrous sodium sulphate. Distilled the toluene under reduced pressure and the solid obtained was recrystallized by using acetone to afford the faint yellow 7-methoxy-2-phenyl-1-benzofuran-5-carbaldehyde (0.40 g, 49 %), m.p. 142-43°C.

FT-IR (KBr): 3035, 2942, 2844, 2721, 1691, 1592, 1475, 1342, 1218, 1139, 993, 840, 746, 719 cm^{-1} .

NMR (300 MHz) (CDCl_3 ; δ ppm) $\text{C}_{16}\text{H}_{12}\text{O}_3$ (mol. Wt. 252.264 g/mol): 4.10 (s, 3H); 7.11 (s, 1H); 7.36-7.94 (m, 7H); 10.01 (s, 1H, -CHO).

Mass Spectra (M + 1): 253.13

2.3.1 Generation of docking sites:

The binding sites for the docking are generated by using Glide software. The site of the protein having more site score is considered for the docking of ligand. The site which has maximum *site points*, located on the site in different colours as hydrophobic and hydrophilic maps. The hydrophilic maps are further divided into donor, acceptor, and metal-binding regions. Other properties characterize the binding site in terms of the size of the site, degrees of enclosure by the protein and exposure to solvent, tightness with which the site points interact with the receptor, hydrophobic and

hydrophilic character of the site and the balance between them, and degree to which a ligand might donate or accept hydrogen bonds. All these properties are summarised in table 5.

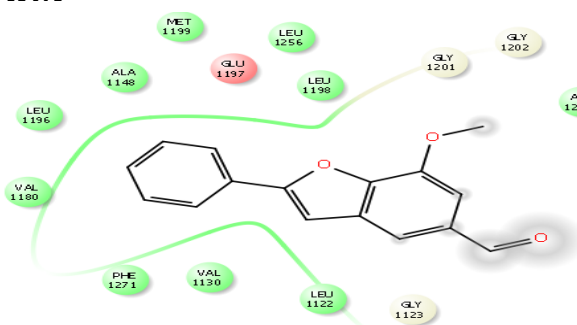
The docking site scores, size, volume exposure, enclosure, contact, hydrophobic and hydrophilic nature, donor and acceptor ratio of all proteins are shown in table 5.

2.3.2 Molecular docking:

The estimation of binding affinity of the ligand-receptor/protein complex is still a challenging task.

Scoring functions (docking score) in docking programs take the ligand-receptor/protein poses as input and provides ranking or estimation of the binding affinity of the pose. These scoring functions require the availability of receptor/protein-ligand complexes with known binding affinity and use the sum of several energy terms such as *van der Waals* potential, electrostatic potential, hydrophobicity and hydrogen bonds in binding energy estimation. The second class consists of *force field-based scoring functions*, which use atomic force fields used to calculate free energies of binding of ligand-receptor/protein complex.

4FNY



1VOM

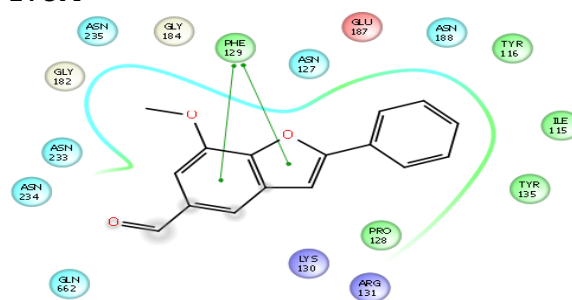
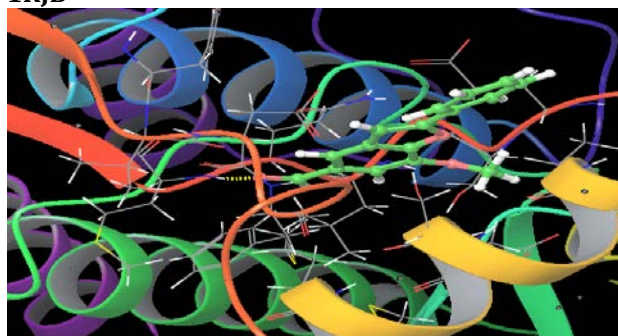
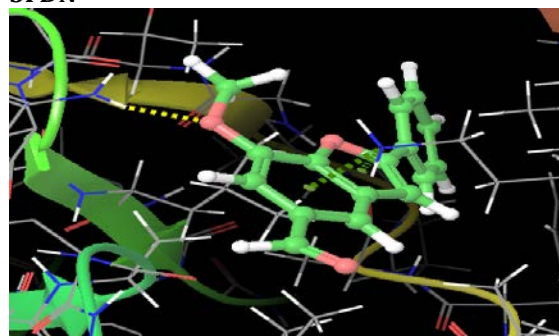


Figure 1: 2D docking image of 7-methoxy-2-phenyl-1-benzofuran-5-carbaldehyde with different proteins

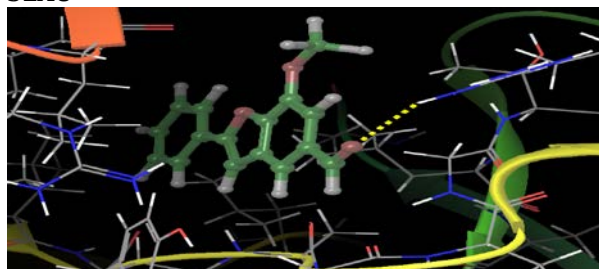
1RJB



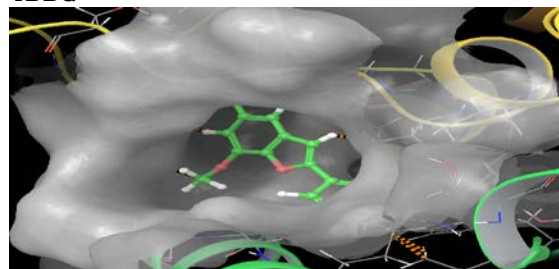
3FDN



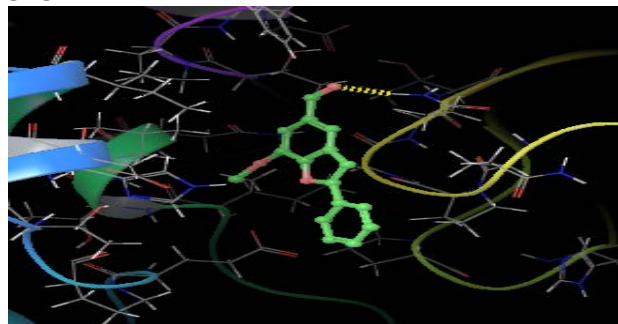
3LAU



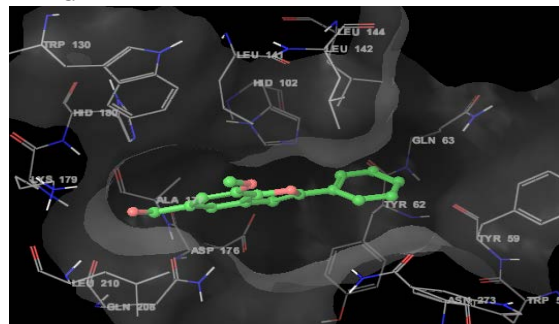
4BBG



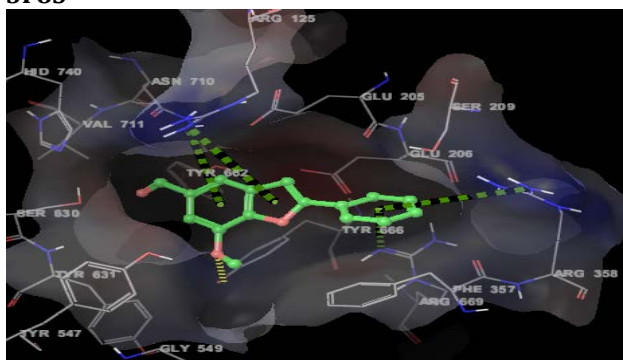
3V3M



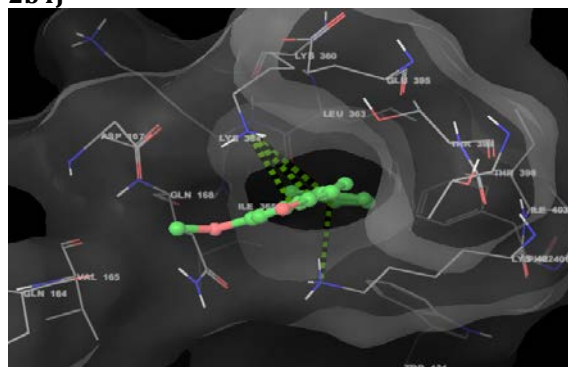
1BAG



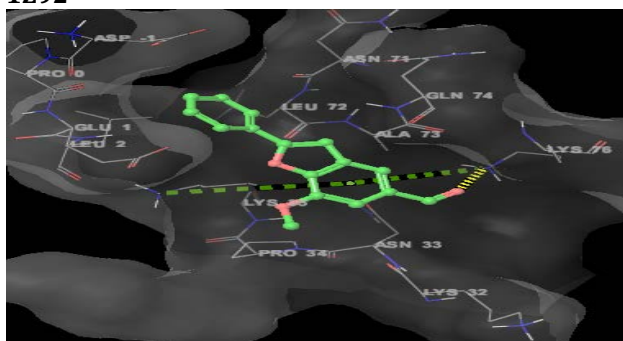
3F8S



2b4J



1Z92



1YCR

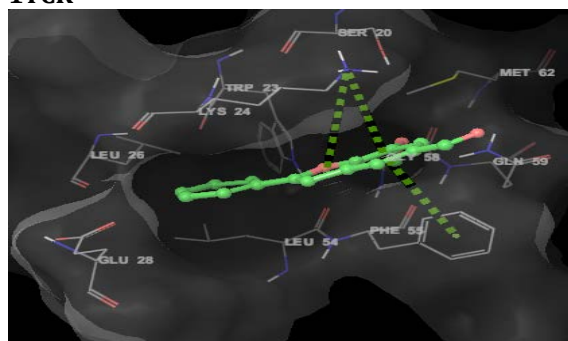


Figure 2: 3D docking image of 7-methoxy-2-phenyl-1-benzofuran-5-carbaldehyde with different proteins

RESULTS AND DISCUSSION

The docking site score of 2AZ1 (1.121) is higher while that of 2BOU (0.464) is lowest which indicates that the 2AZ1 protein is more favourable for docking than the others. The size (223) and volume (760.774) available for docking is higher in 4BBG and 3FDN PDBs respectively but exposure to the ligand as compared to 2BOU is lower. The exposure to the ligand is maximum in 2BOU and minimum in 2AZ1 while reverse is the case for the enclosure area, it is higher in 2AZ1 and minimum in 2BOU. The overall contact area to the ligand is higher in 1RJB (1.124). The hydrophobic nature or character and balance between hydrophobic and hydrophilic nature of the active site is higher in 4FNY and 2b4J respectively while that of lower in 1TE6. The hydrophilic nature or character of the active site is higher in 2AZ1 and lower in 4FNY. The ligands having more hydrophilic nature binds more tightly with 1TE6 and weak binding is observed with to 4FNY (according to the hydrophobic to hydrophilic ratio i.e. balance is higher in 4FNY than lower in 1TE6).

The order of proteins in the decreasing order of hydrophilic character and increasing order of hydrophobic character is – 1TE6 > 2BOU > 2AZ1 > 3F8S > 1BAG > 1KDR > 1P62 > 3V3M > 1Z92 > 1UFQ > 1RJB > 3FDN > 3MK2 > 4BBG > 1VOM > 3LAU > 1YCR > 2b4J > 4FNY. This indicates that ligands with more hydrophobic nature bind easily to 4FNY. The hydrogen bond donor/acceptor character ratio is higher in 1YCR (2.006) while lower in 1BAG (0.478) therefore the ligand contains more hydrogen bond acceptor atoms/groups binds more tightly binds to 1YCR than those containing hydrogen bond donor atoms/groups

bind to 1BAG. The order protein in the decreasing order of H-bond donor to H-bond acceptor ratio is – 1YCR > 4FNY > 2b4J > 2BOU > 1Z92 > 1UFQ > 3FDN > 3F8S > 3LAU > 4BBG > 1VOM > 1RJB > 2AZ1 > 1KDR > 3MK2 > 1TE6 > 1P62 > 3V3M > 1BAG.

The docking score table 1A and 1B and table 2 indicate 7-methoxy-2-phenyl-1-benzofuran-5-carbaldehyde is more active against 1VOM and 4FNY while is less active against 1RJB and 2b4J. There are number of types of interactions observed between ligand and receptor such as hydrogen bonding, pi-pi interactions, ion-pi interactions, hydrophobic and hydrophilic interactions, ionic interactions, van der Waal interactions, etc along with steric interactions determine the docking score.

Glide esite explains the polar interaction in the active site between ligand and amino acid residue at the docking site after recombination. The polar interactions between the aldehyde and amino acid residues of the protein are only observed in 1UFQ (-0.066), 1KDR (-0.015), 3MK2 (-0.010), 1TE6 (-0.045) and 1P62 (-0.083) but not observed in 1VOM and 4FNY. The aldehyde shows higher polar interaction 3MK2, 1VOM, 1TE6, 1BAG, and 3V3M proteins PDB. Such types of interactions are not observed in 3LAU, 4BBG, 4FNY and 1UFQ. Therefore, the docking score of aldehyde is comparatively higher in 4FNY. This is one of the reason for high docking score of aldehyde during docking with 4FNY (even though there is absence of hydrogen bonding and stronger pi-cation/anion interactions).

The aldehyde does not have any hydrogen atom which is capable of forming L (ligand)→P (protein) hydrogen bonding. It contains sp² and sp³ hybridised oxygen atoms (carbonyl, ether and aromatic) capable of

forming P → L type of hydrogen bonding during interaction. The backbone of MET and GLY amino acids and side chain atoms of ARG, TYR, ASN, GLN and LYS formed H-bonding with ligand.

Table 1A: Docking properties of 7-methoxy-2-phenyl-1-benzofuran-5-carbaldehyde with different receptor or protein PDBs.

Description	Protein									
	1RJB	3FDN	3LAU	4BBG	3V3M	1BAG	3F8S	2b4J	1Z92	1YCR
Potential Energy OPLS 2005	63.077	63.077	63.077	63.077	63.077	63.077	63.077	63.077	63.077	63.077
RMS Derivative OPLS 2005	0.042	0.042	0.042	0.042	0.042	0.042	0.042	0.042	0.042	0.042
Glide lignum	4	4	1	3	4	7	2	2	7	7
Docking Score	-6.068	-5.41	-6.648	-6.053	-3.095	-5.946	-4.845	-3.861	-5.272	-4.909
Glide Ligand efficiency	-0.319	-0.285	-0.35	-0.319	-0.163	-0.313	-0.255	-0.203	-0.277	-0.258
Glide Ligand efficiency sa	-0.852	-0.76	-0.934	-0.85	-0.435	-0.835	-0.68	-0.542	-0.74	-0.689
Glide Ligand efficiency In	-1.538	-1.372	-1.685	-1.535	-0.785	-1.507	-1.228	-0.979	-1.336	-1.245
Glide gscore	-6.068	-5.41	-6.648	-6.053	-3.095	-5.946	-4.845	-3.861	-5.272	-4.909
glide lipo	-1.795	-1.254	-2.302	-1.758	0.46	-1.984	-0.663	-0.32	-1.662	-1.571
glide hbond	-0.587	-0.35	-0.043	0	0	0	-0.355	-0.035	-0.041	-0.157
glide metal	0	0	0	0	0	0	0	0	0	0
glide rewards	-1.848	-1.324	-2.872	-1.788	-1.992	-2.364	-1.926	-1.992	-1.889	-1.779
Glide evdw	-33.092	-27.851	-30.119	-33.289	-21.256	-29.459	-23.812	-25.904	-26.543	-26.483
Glide ecoul	-3.058	-3.191	-1.902	-0.846	-2.021	-2.672	-6.57	-3.292	-4.187	-2.362
glide erotb	0.276	0.276	0.276	0.276	0.276	0.276	0.276	0.276	0.276	0.276
glide esite	0	0	0	0	0	0	0	0	0	0
Glide emodel	-45.747	-36.672	-45.342	-38.317	-32.675	-43.305	-34.845	-35.429	-40.203	-34.285
Glide energy	-36.150	-31.042	-32.021	-34.135	-23.277	-32.131	-30.382	-29.196	-30.730	-28.845
Glide einternal	7.172	1.592	0.191	9.274	0.074	1.738	9.635	0.56	1.986	5.884
glide confnum	1	1	1	1	1	1	1	1	1	1
Glide posenum	194	4	359	2	1	346	313	78	253	294
XP GScore	-6.068	-5.41	-6.648	-6.053	-3.095	-5.946	-4.845	-3.861	-5.272	-4.909
HBond	1	1	1	0	1	0	1	0	1	0
Pi-Pi interactions	1	0	0	0	0	0	0	0	0	1

Table 1B: Docking properties of 7-methoxy-2-phenyl-1-benzofuran-5-carbaldehyde with different receptor or protein PDBs.

Description	Protein								
	4FNY	2BOU	1UFQ	1VOM	2AZ1	1KDR	3MK2	1TE6	1P62
Potential Energy OPLS 2005	63.077	63.077	63.077	63.077	63.077	63.077	63.077	63.077	63.077
RMS Derivative OPLS 2005	0.042	0.042	0.042	0.042	0.042	0.042	0.042	0.042	0.042
Glide lignum	2	2	2	2	2	2	2	2	2
Docking Score	-6.843	-4.216	-4.531	-6.921	-4.786	-4.069	-4.752	-3.963	-4.393
Glide Ligand efficiency	-0.360	-0.222	-0.238	-0.364	-0.252	-0.214	-0.25	-0.209	-0.231
Glide Ligand efficiency sa	-0.961	-0.592	-0.636	-0.972	-0.672	-0.572	-0.667	-0.557	-0.617
Glide Ligand efficiency In	-1.735	-1.069	-1.149	-1.755	-1.213	-1.032	-1.205	-1.005	-1.114
Glide gscore	-6.843	-4.216	-4.531	-6.921	-4.786	-4.069	-4.752	-3.963	-4.393
glide lipo	-3.621	-1.457	-1.343	-3.024	-0.743	-0.452	-2.063	-0.204	-0.551
glide hbond	0	-0.026	-0.113	-0.263	-0.228	-0.3	0	-0.439	-0.199
glide metal	0	0	0	0	0	0	0	0	0
glide rewards	-1.966	-1.721	-1.689	-1.998	-2.065	-1.689	-1.689	-1.689	-1.689
Glide evdw	-28.922	-23.618	-27.208	-30.434	-30.964	-26.193	-25.188	-22.553	-26.996
Glide ecoul	-0.567	-0.718	-1.563	-2.597	-3.177	-3.867	-0.036	-4.895	-5.308
glide erotb	0.276	0.276	0.276	0.276	0.276	0.276	0.276	0.276	0.276
glide esite	0	0	-0.066	0	0	-0.015	-0.01	-0.045	-0.083
Glide emodel	-41.888	-30.525	-36.783	-46.554	-42.436	-37.744	-32.741	-34.619	-41.304
Glide energy	-29.488	-24.336	-28.771	-33.030	-34.141	-30.060	-25.225	-27.448	-32.304
Glide einternal	0.199	0.407	1.189	0.664	3.986	0.882	0.428	0.429	1.655
glide confnum	1	1	2	2	1	1	1	2	2
Glide posenum	196	312	154	22	213	51	325	311	350
XP GScore	-6.843	-4.216	-4.531	-6.921	-4.786	-4.069	-4.752	-3.963	-4.393
H-Bonds	0	0	0	0	1	1	0	2	1
Pi-Pi interactions	0	0	0	2	0	4	0	4	2

Glide evdw explains the van der Waal energy of the complex of ligand and amino acid residue at the docking site after recombination. The comparison between glide evdw and glide energy shows that van der Waal energy shows major contribution than coulombic energy for the stabilisation of complex. The van der Waal interaction depends on surface area (polar and non-polar) of the ligand, as surface area increases, van der Waal energy increases and vice

versa. The contribution of glide evdw into the docking score is considerable. The Glide evdw of the interaction in decreasing order is 4BBG > 1RJB > 2AZ1 > 1VOM > 3LAU >

Glide energy is summation of coulomb and van der Waal energy of interaction. The glide energy table 3 indicates that, the comparatively coulombic force and van der Waal interactions (energies) are higher for the

aldehyde-1RJB complex. This is due to higher surface area (both polar and non-polar) of 1RJB available for interaction with aldehyde. The aldehyde has higher glide energy during the interaction with PDBs in the decreasing order as 1RJB > 2AZ1 > 4BBG > 1VOM > 1P62 > 1BAG > 3LAU >

Along with major interactions, there are some other interactions such polar interactions (faint blue colour), hydration sites (orange, interaction with water), electrostatic interactions (blue and pink) and hydrophobic interaction (major weak interaction with maximum number of amino acids) present between the ligand-protein complex.

The table 3 (Electrostatic interactions (blue)) shows that, two amino acids in all proteins such as ARG and LYS showed positive interactions (hydrogen bonding between proton of protein and O/N of ligand or electrostatic interaction between positive centre of protein and negative / electron density of ligand). Both the amino acids containing amino group in their side chain which is capable of forming such type of interactions in neutral or protonated forms. Benzofuran aldehyde showed stronger such interaction with same amino acids of 1P62, 1TE6, 1KDR, 1AZ1, 1Z92, 2b4J, and 3F8S indicates that orientation of the molecule does not change during docking in major extended by the changing of skeleton or functional group. But such type of interactions are absent with 3MK2, 4FNY and 3V3M.

The table 3 (Electrostatic interactions (pink)) shows that, two amino acids in all proteins viz. ASP and GLU shows negative interactions (hydrogen bonding between proton of ligand and oxygen of protein or electrostatic interaction between positive centre of ligand and negative / electron density of protein). Both the amino acids containing carboxylic acid group in their side chain which is capable of forming such type of interactions in neutral or deprotonated form. This type interaction depends on the number of positive charge centre present in the ligand molecules and number of donor amino acids present in the docking site. 1RJB, 4BBG, 1UFQ, 3FDN, 2AZ1, and 1P62 PDBs shows maximum number of such type of interactions with aldehyde while 1YCR, 3LAU, 3V3M, 1BAG, 4FNY, 1VOM and 3MK2 shows minimum number of such interactions.

Benzofuran aldehyde molecule is hydrophobic in nature, even though it has strong region for hydrogen bonding, pi-pi interactions and hydrophobic interactions. This interaction would trigger the change in orientation of structure and their groups during binding. The group of aldehyde such as C=O, -O-, aromatic -O- groups/atoms are capable for the formation of hydrogen bonding. The aromatic ring and -CH₃ group force some limitations in the packing of micellar rearrangement as well as reducing the chance of forming hydrogen bonding with amino acids residue of protein.

Table 2: Table of don/acc ratio, docking score, glide esite and polar interactions of 7-methoxy-2-phenyl-1-benzofuran-5-carbaldehyde with different receptor or protein PDBs.

Proteins	Description of property and amino acid information					
	don/acc at the docking site	at the Docking score	the Docking score	Glide esite	No. of hydrogen bonds (amino acid residues)	Polar interactions (amino acid residues) (π - π , π -cation)
1RJB	0.706	-3.095	0	0	01 (MET578) (with backbone)	SER274, SER660, GLN577
3FDN	0.880	-6.053	0	0	01 (ASN261) (with side chain)	ASN261, THR217
3LAU	0.749	-6.648	0	0	01 (ARG220) (with side chain)	--
4BBG	0.725	-5.41	0	0	--	--
3V3M	0.510	-6.068	0	0	01 (GLN110) (with side chain)	GLN107, GLN110, ASN203, ILE246, THR292
1BAG	0.478	-5.946	0	0	--	GLN63, GLN208, HID102, HIG180, ASN273
3F8S	0.762	-4.845	0	0	01 (TYR666) (with side chain)	SER209, SER263, ASN710, HID740
2b4J	1.456	-3.861	0	0	--	C-THR398, C-THR399, A-GLN164, A-GLN168
1Z92	1.427	-5.272	0	0	01 (A-LYS261) (with side chain)	A-ASN33, A-ASN71, A-GLN74
1YCR	2.006	-4.909	0	0	--	B-SER20, A-GLN59
4FNY	1.858	-6.843	0	0	--	--
2BOU	1.433	-4.216	0	0	--	SER28, SER29, SER31
1UFQ	0.931	-4.531	-0.066	0	--	--
1VOM	0.708	-6.921	0	0	--	ASN127, ASN188, ASN233, ASN234, ASN235, GLN662
2AZ1	0.665	-4.786	0	0	01 (A-ARG19) (with side chain)	B-THR27, B-THR31
1KDR	0.661	-4.069	-0.015	0	01 (GLY19) (with backbone)	SER14, SER101
3MK2	0.623	-4.752	-0.01	0	--	THR124, HID162, THR163, GLN184, GLN189, SER192, ASN193
1TE6	0.595	-3.963	-0.045	0	02 (B-LYS59, B-ASN16) (with side chain)	A-HID189, B-ASN16, B-SER39, B-SER156, B-HID157
1P62	0.520	-4.393	-0.083	0	01 (ARG128) (with side chain)	SER35, THR36

Table 3: Table of glide evdw, glide energy, electrostatic and polar interactions of 7-methoxy-2-phenyl-1-benzofuran-5-carbaldehyde with different receptor or protein PDBs.

Proteins	Description of property and amino acid information					
	Glide evdw	Glide energy	Electrostatic interactions (blue)	Electrostatic interactions (pink)	Polar interactions (amino acid residues)	
1RJB	-33.092	-36.150	ARG595	GLU573, GLU661, GLU656, ASP593	SER274, SER660, GLN577	
3FDN	-27.851	-31.042	LYS162	GLU211, GLU260, ASP274	ASN261, THR217	
3LAU	-30.119	-32.021	ARG137, ARG220	GLU211	--	
4BBG	-33.289	-34.135	ARG119, ARG221	GLU116, GLU118, GLU215, ASP130	--	
3V3M	-21.256	-23.277	--	GLU240	GLN107, GLN110, ASN203, ILE246, THR292	
1BAG	-29.459	-32.131	LYS179	ASP176	GLN63, GLN208, HID102, HIG180, ASN273	
3F8S	-23.812	-30.382	ARG125, ARG358, ARG669	GLU250, GLU206	SER209, SER263, ASN710, HID740	
2b4J	-25.904	-29.196	C-LYS360, C-LYS364, C-LYS402	A-ASP167, C-GLU395	C-THR398, C-THR399, A-GLN164, A-GLN168	
1Z92	-26.543	-30.730	A-LYS32, A-LYS35, A-LYS76	B-GLU1, B-ASP-1	A-ASN33, A-ASN71, A-GLN74	
1YCR	-26.483	-28.845	B-LYS24	B-GLU28	B-SER20, A-GLN59	
4FNY	-28.922	-29.488	--	GLU1197	--	
2BOU	-23.618	-24.336	ARG22	GLU32, GLU46	SER28, SER29, SER31	
1UFQ	-27.208	-28.771	C-LYS190, D-LYS202	C-GLU194, C-GLU195, D-GLU194, D-GLU195	--	
1VOM	-30.434	-33.030	LYS130, ARG131	GLU187	ASN127, ASN188, ASN233, ASN234, ASN235, GLN662	
2AZ1	-30.964	-34.141	A-ARG19, B-ARG147, E-ARG19	A-ASP24, A-GLU30, E-ASP24	B-THR27, B-THR31	
1KDR	-26.193	-30.060	LYS18, ARG41, ARG131, ARG181	ASP35, ASP129	SER14, SER101	
3MK2	-25.188	-25.225	--	GLU28	THR124, HID162, THR163, GLN184, GLN189, SER192, ASN193	
1TE6	-22.553	-27.448	A-LYS192, B-ARG14, B-ARG49, B-LYS59	B-GLU47, B-ASP208	A-HID189, B-ASN16, B-SER39, B-SER156, B-HID157	
1P62	-26.996	-32.304	LYS34, ARG128, ARG188, ARG192, ARG194	GLU53, GLU127, GLU197	SER35, THR36	

Table 4: Table of glide lipo and polar interactions of 7-methoxy-2-phenyl-1-benzofuran-5-carbaldehyde with different receptor or protein PDBs, hydrophobic and hydrophilic character of PDBs.

Proteins	Description of property and amino acid information				
	phobic	philic	Glide lipo	Pi-pi interactions (green)	Pi-cation interactions (pink)
1RJB	0.668	1.186	-1.795	ARG595	--
3FDN	0.758	1.170	-1.254	--	LYS162 (2 rings)
3LAU	1.245	0.819	-2.302	--	--
4BBG	1.274	1.108	-1.758	--	--
3V3M	0.473	1.200	0.46	--	--
1BAG	0.343	1.103	-1.984	--	--
3F8S	0.298	1.089	-0.663	--	ARG125, ARG358, ARG669
2b4J	1.321	0.765	-0.320	--	C-LYS360 (2 rings), C-LYS402
1Z92	0.396	0.805	-1.662	--	A-LYS35, A-LYS78
1YCR	1.171	0.675	-1.571	A-PHE55	B-LYS24
4FNY	1.470	0.654	-3.621	--	--
2BOU	0.134	1.000	-1.457	--	--
1UFQ	0.51	0.947	-1.343	--	--
1VOM	1.022	0.853	-3.024	PHE-129 (02)	--
2AZ1	0.397	1.562	-0.743	--	--
1KDR	0.463	1.343	-0.452	ARG-41, ARG-131 (02 each)	--
3MK2	0.632	0.717	-2.063	--	--
1TE6	0.008	1.703	-0.204	ARG-14, ARG-49 (02 each)	B-ARG-14 (01)
1P62	0.49	1.393	-0.551	ARG-194 (02)	LYS-34 & ARG-194 (01 each)

Glide lipo explains the lipophilic and lipophobic attraction between ligand and amino acid residue at the docking site after recombination. The molecule is undissociated and thus available for penetration through various lipid barriers. The rate of penetration is strongly depends on the lipophilicity of the drug molecule in its unionised form. The lipophilic-hydrophilic balance plays very important role in passive transport and active transport along with drug metabolism. As length of hydrophobic chain increases,

both partition coefficient and anaesthetic potency increases. Lipophilic and phobic attraction between aldehyde and amino acid residue at the docking site is stronger in 1VOM, 3LAU and 3MK2 PDBs at the neutral pH = 7. At lower pH, amine get protonated and its lipophilicity character goes on decreasing. The aldehyde shows weaker lipophilic and hydrophobic attraction with 1TE6, 4b4J, 1FDR, 3V3M, 1P62, and 2AZ1.

Table 5: Docking site score and other properties of docking site of different PDBs.

protein	Site Score	size	Dscore	volume	exposure	enclosure	contact	phobic	philic	balance	don/acc
3V3M	0.913	75	0.852	258.279	0.611	0.715	0.927	0.473	1.200	0.395	0.510
4BBG	1.040	223	1.034	503.867	0.522	0.758	1.035	1.274	1.108	1.150	0.725
3LAU	1.046	116	1.095	437.325	0.609	0.703	0.883	1.245	0.819	1.520	0.749
3FDN	1.047	206	1.02	760.774	0.531	0.768	0.964	0.758	1.170	0.648	0.880
1RJB	1.073	100	1.037	195.51	0.492	0.807	1.124	0.668	1.186	0.563	0.706
1BAG	0.989	143	0.989	425.663	0.676	0.681	0.849	0.343	1.103	0.311	0.478
3F8S	1.009	146	1.012	489.118	0.647	0.711	0.855	0.298	1.089	0.274	0.762
2b4J	1.074	121	1.136	552.321	0.752	0.728	0.860	1.321	0.745	1.773	1.456
1Z92	0.961	95	1.013	316.246	0.749	0.599	0.699	0.396	0.805	0.492	1.427
1YCR	0.755	41	0.754	90.552	0.653	0.620	0.849	1.171	0.675	1.735	2.006
1TE6	1.05	193	0.849	507.64	0.515	0.773	0.993	0.008	1.703	0.004	0.595
1VOM	1.074	222	1.114	618.772	0.605	0.754	0.934	1.022	0.853	1.198	0.708
2BOU	0.464	16	0.375	45.962	0.807	0.542	0.727	0.134	1.000	0.134	1.433
3MK2	0.872	73	0.914	179.389	0.731	0.574	0.712	0.632	0.717	0.882	0.623
1KDR	1.047	276	0.963	749.112	0.472	0.768	1.009	0.463	1.343	0.345	0.661
1P62	1.048	200	0.948	372.841	0.438	0.770	1.007	0.49	1.393	0.352	0.520
1UFQ	1.009	176	1.042	756.315	0.656	0.684	0.862	0.51	0.947	0.538	0.931
2AZI	1.121	150	0.958	367.01	0.385	0.879	1.096	0.397	1.562	0.254	0.665
4FNY	1.092	195	1.161	426.349	0.556	0.724	0.932	1.470	0.654	2.249	1.858

The electron rich pi-system (containing electron donating group) generally interact with other electron deficient pi-system having electron withdrawing group. These are denoted by green colour and are called as hydrophobic interactions. Also, electron rich pi-centre interacts with cation (denoted by dark blue colour) and electron deficient centre interact with anion (denoted by pink colour). The benzofuran aldehyde shows the pi-pi interactions with the amino acid residue containing aromatic ring or pi electrons, the amino acids such as ARG (C=N bond) and PHE shows such interactions with aldehyde. The pi-cation interaction are shown by those amino acid residue containing free cation or partial

positive charge centre in their side chain such as LYS and ARG, both containing amino groups which get protonated and forming quaternary ammonium cation which interact with pi-electrons of aldehyde. The polar hydroxyl group (hydrogen having partial positive charge/oxygen having partial negative charge/lone pair of electrons of oxygen) interact with aromatic ring. These types of interactions depend on the orientation of the molecule in the docking site and amino acid arrangement in the same. The 7-methoxy-2-phenyl-1-benzofuran-5-carbaldehyde shows strong interactions with cancer proteins.

Table 6A: Molecular properties of aldehyde

mol MW	dipole	SASA	Donor HB	Accept HB
252.269	6.261	499.19	0	3.25
Potential Energy- OPLS-2005	RMS Derivative- OPLS-2005	volume	dip ² /V	Glob
63.077	0	845.27	0.046369	0.86609
FOSA	FISA	PISA	WPSA	ACxDN ^{0.5} /SA
99.71	76.339	323.141	0	0
QPpolarz	QPlogPC16	QPlogPoct	QPlogPw	QPlogPo/w
29.475	8.871	11.879	6.398	3.077
QPlogS	CIQPlogS	QPlogHERG	QPPCaco	QPlogBB
-3.65	-3.822	-5.24	1870.603	-0.236
QPPMDCK	QPlogKp	IP(eV)	Human Oral Absorption	Percent Human Oral Absorption
973.487	-1.596	8.84	3	100
SAfluorine	SAamideO	PSA	#NandO	Rule Of Five
0	0	51.581	3	0
Rule Of Three	EA(eV)	#metab	QPlogKhsa	#ringatoms
0	0.733	2	0.118	15
#in34	#in56	#noncon	#nonHatm	Jm
0	15	0	19	1.433

Table 6B: Molecular properties of aldehyde

Stretch energy	Kcal/mole	01.3402
Bend energy	Kcal/mole	15.4091
Stretch-Bend energy	Kcal/mole	00.1248
Torsion energy	Kcal/mole	-17.7538
Non-1,4 VDW	Kcal/mole	00.5944
1,4 VDW	Kcal/mole	17.8430
Dipole/Dipole	Kcal/mole	01.2730
Total Energy	Kcal/mole	18.8306
Stereochemistry		C(8)-C(7): (Z)
Boiling point	K ± 25	667.848

Critical Pressure	Bar	27.556
Critical Temperature	K	886.858
Critical Volume	cm ³ /mol	715.5
Gibbs Free Energy	kJ/mol	77.92
Heat of Formation	kJ/mol	-145.27
Henry's Law Constant		6.614
Ideal Gas Thermal Capacity		265.045
LogP		2.999
Melting Point	K ± 25	486.24
Mol Refractivity	cm ³ /mol	72.967
Vapor Pressure	Pascal	0
Water Solubility	Mg/lit	0
Log (p)	By Crippen's fragmentation ± 0.47	3.00
Log (p)	By Viswanadhan's fragmentation ± 0.49	2.87
MR	By Crippen's fragmentation (cm ³ /mol) ± 1.27	74.01
MR	By Viswanadhan's fragmentation (cm ³ /mol) ± 0.77	72.97
H	Log[unitless]	6.614 ± 0.340
LogP	Log unit	3.6383
Log S	Log unit	-4.1243
Lipinski Rule		252.079; 3; 0; 3; 4.437
Formal Charge		0
Connolly Accessible Area	A2	466.969
Connolly Molecular Area	A2	231.696
Connolly Solvent Excluded Volume	A3	188.76
Mol Formula		C16H12O3
Exact Mass	g/mol	252.0786
Mol. Weight	g/mol	252.269
Number of HBond Acceptors		3
Number of HBond Donors		0
Ovality		1.455999
Principal Moment		512.724 2482.469 2991.739
Elemental Analysis		C - 76.18; H - 4.79; O - 19.03
m/z	(contain intensity of peak)	252.08 (100), 253.08 (17.3), 254.09 (1.4)
Mol Refractivity		7.218099
Partition Coefficient		4.436800
Balaban Index		136390
Cluster Count		19
Molecular Topological Index		5220
Num Rotatable Bonds	Bonds	3
Polar Surface Area	A2	35.53
Radius	Atoms	5
Shape Attribute		17.0526315
Shape Coefficient		1
Sum Of Degrees		42
Sum Of Valence Degrees		70
Topological Diameter	Bonds	10
Total Connectivity		0.0008184
Total Valence Connectivity		7.577876
Wiener Index		691
UV spectra		
HOMO → LUMO + 1	Peak:	214.98
	Intensity:	0.11724
HOMO → LUMO	Peak:	234.00
	Intensity:	0.93253
HOMO -4/5 → LUMO +1	Peak:	284.41
	Intensity:	0.0002
Energy of HOMO	eV	-11.462
Energy of LUMO	eV	-04.476
Energy of LUMO+1	eV	-01.133
Huckel Charge:	Aldehydic C	0.356604
	Aldehydic O	-0.527568
	Furan ring O	0.115297
Lowdin Charge:	Aldehydic C	0.189149
	Aldehydic O	-0.263668
	Furan ring O	-0.071562
Mulliken Charge:	Aldehydic C	0.401810
	Aldehydic O	-0.567947
	Furan ring O	-0.798507
By using Lipinski rule of five		
Molecular weight	Dalton	252.265

No. of H-bond acceptor	(< 10)	03
No. of H-bond donor	(< 5)	00
Virtual Log P	(< 5)	3.968
Comment		Ok
By using Ghose's rule of five		
Molecular weight	Dalton	252.265
Number of atoms	20 – 70	31
Virtual Log P	-0.4 – 5.6	3.968
Molar refractivity	40 – 130	73.9344
Comment		Ok

Acknowledgments

The authors are grateful to the Principal and Head, Government of Maharashtra, Ismail Yusuf Arts, Science and Commerce College, Mumbai 60, India, and Principal and Head, Department of Chemistry, Patkar Varde College, Goregaon (W), Mumbai, India for his constant encouragement. For the spectral analyses and characterization, basic facilities and helpful discussions during the synthesis the authors are thankful to Ram Jadhav, Dr. Dileep Khandekar, Dr. D D Patil. The authors are especially thankful to Schrodinger software company group for their help and support.

REFERENCES

1. Leach, A. R. Molecular Modelling: Principles and Applications, Second Edition, Published by Pearson Education EMA, January 2001.
2. Ooms, F. (2000). Molecular modelling and computer aided drug design. Examples of their applications in medicinal chemistry. *Curr. Med. Chem.* 7(2):141-158.
3. Halperin I, Ma B, Wolfson H et al. (2002). Principles of docking: An overview of search algorithms and a guide to

scoring functions. *PROTEINS: Structure, Function, and Genetics*, 47:409-443.

4. *Acc Chem Res* 1996; 29: Several articles in issue 3.
5. Fernandes P. B. (1998). Technological advances in high-throughput screening. *Curr Opin Chem Biol* 2:597-603.
6. Hertzberg RP, Pope AJ. (2000). High-throughput screening: New technology for the 21st century. *Curr Opin Chem Biol* 4:445-451.
7. Clark DE. (2005). Computational prediction of ADMET properties: Recent developments and future challenges. *Annu Rep Comput Chem* 1:133-151.
8. Babu R Thorat; Dyneshwar Shelke; Ramdas Atram et al. (2013). Wittig reaction approach for the synthesis of 7-methoxy-2-[4-alkyl/aryl]-1-benzofuran-5-carboxaldehyde, *Het. Lett.* 3(3):385-396.

© 2015; AIZEON Publishers; All Rights Reserved

This is an Open Access article distributed under the terms of the Creative Commons Attribution License which permits unrestricted use, distribution, and reproduction in any medium, provided the original work is properly cited.
